Asian Journal of Chemistry; Vol. 33, No. 12 (2021), 2972-2976

ASIAN JOURNAL OF CHEMISTRY

https://doi.org/10.14233/ajchem.2021.23425

Optical Studies of Organically Functionalized Mn doped ZnS Quantum Dots

ANJU BALA[1,*], RAJEEV SEHRAWAT[1], RENU BALA[2] and ASHUTOSH DIXIT[2]

[1]Department of Physics, Maharishi Markandeshwar (Deemed to be) University, Mullana-133203, India
[2]Department of Chemistry, Maharishi Markandeshwar (Deemed to be) University, Mullana-133203, India

*Corresponding author: E-mail: anjukamboj134@gmail.com

Received: 21 July 2021; *Accepted*: 30 August 2021; *Published online*: 6 December 2021; AJC-20587

Organically functionalized manganese doped zinc sulfide (ZnS/Mn) quantum dots were prepared by simple chemical method with polypyrrole (PPy) used as a capping agent. Prepared quantum dots were characterized with Fourier transform infrared spectroscopy (FTIR), high resolution transmission electron microscopy (HR-TEM), X-ray diffraction microscope (XRD), UV-visible spectroscopy and photoluminescence spectroscopy. Crystalline size of PPy capped ZnS/Mn quantum dots for various concentrations of PPy were approximate 2 nm as analyzed by XRD and TEM analysis. The absorption spectra revealed the occurrence of a blue shift in the peak of absorption and an increase in the band gap value due to the quantum confinement effect. FTIR spectroscopy confirmed that shifting of broad peak at 2335.8 cm^{-1} was due to S-H stretching vibrations, which confirmed interaction of hydrogen and sulphur in ZnS/Mn/PPy nanocomposites. Uncapped ZnS/Mn and PPy capped ZnS/Mn quantum dots reveal the effective photoluminescence emission spectra in the range of 300-700 nm. With increase the value of capping agent in ZnS/Mn quantum dots, photoluminescence spectra going to red shifting. The photoluminescence properties of the organically functionalized ZnS nanoparticles are favourable for the application in optoelectronic devices.

Keywords: ZnS/Mn nanoparticles, Organically functionalized, Quantum confinement effect, Optical properties.

INTRODUCTION

Semiconductors of group II-VI are evincing great interest among the various research groups across the world, because of their size-dependent properties, as a consequence of strong quantum confinement effect. The quantum confinement effect occurs in nanoparticles if the particle size is less than the exciton radius of Bohr. If such is the case, the nanoparticles are transformed into quantum dots. Zinc sulfide (ZnS) is one of well-known semiconductor material having different fundamental properties like band gap of 3.68 eV at room temperature, high refractive index and high transmittance for the visible region - this provides promising scope for its potential applications including flat panel displays [1], optoelectronic devices, bio devices [2], infrared windows [3], light emitting diode [4] and other electroluminescence devices [5].

Different studies on doped ZnS nanoparticles have been performed by the researchers to improve the optical and structural properties. For example Ag, Pd, Fe, Cu Mg, Zr and Mn doped ZnS nanostructures have gained significant research interest in the last two decades [6-9] in order to enhance the properties of ZnS nanoparticles. Due to the many applications of Mn doped ZnS, several researches investigated the structural and optical properties of nanocrystals [10,11]. When Mn ions are included in the ZnS matrix, the forbidden transition of $4T_1$-$6A_1$ is enabled, resulting in the emission characteristics of Mn. Also the few researchers indicated that the capping can further enhance certain optical, electrical, magnetic and structural properties of doped ZnS nanoparticles [12,13]. Kuppayee *et al.* [14] studied different properties of copper doped ZnS nanoparticles with using of Tri-*n*-octylphosphine oxide and sodium hexametaphosphate as capping agent. Li *et al.* [15] studied different properties of 3-mercaptopropionic acid (MPA) capped Mn-doped ZnS quantum dots [15]. Singhal *et al.* [16] studied about effect of pyridine capping on optical and morphological properties of Mn doped ZnS quantum dots.

Polypyrrole (PPy) is an organic semiconductor with broad emission spectra from the ultraviolet to the visible region. As

a result, it is a promising candidate for a new class of organic-inorganic composite materials with enhanced light absorption properties [17]. Interactions between inorganic semiconductors and organic polymer can produce interesting properties that differ significantly from individual one. Considering this fact many researchers have been using capped ZnS nanocomposites to achieve structural and optical characteristics. However, no reports on optical properties of organic functionalized Mn doped ZnS quantum dots have been reported.

So far, chemical precipitation method, hydrothermal synthesis, liquid based method, sol-gel method and chemical vapour deputation methods have been studied for the synthesis of ZnS nanoparticles [18-21]. However, both the particle size reduction and cost of production of nanoparticles favours the chemical precipitation method. Other benefits of chemical precipitation method are simple synthesis steps, least material waste, high purity of product material and environment friendly, hence this approach has been used for the synthesis of ZnS and Mn doped ZnS nanoparticles.

In this study, it is aimed to find the structural, optical and morphological properties of organically functionalized ZnS/Mn nanoparticles with various capping concentration of PPy. The structural and morphological properties of nanocomposites were studied using XRD, TEM, FTIR, UV visible and photoluminescence spectroscopy.

EXPERIMENTAL

Zinc acetate (AR 99.5%), sodium sulfide (GR 99%), acetone (GR 99%) and manganese acetate tetrahydrate (GR 99.5%) were obtained from LOBA CHEMIE, $FeCl_3$ (GR 98%), pyrrole azole divinyle extra pure (GR 99%) were bought from SRL.

Synthesis of manganese doped ZnS: Manganese doped ZnS (ZnS/Mn) nanoparticles were synthesized by simple chemical method. Manganese acetate (0.6373 g) was dissolved in 20 mL distilled water by stirring for 30 min. This solution added dropwise to another solution of zinc acetate (11.19 g) in 50 mL distilled water. Sodium sulfide (3.98 g) was mixed in 50 mL of double distilled water and then added dropwise to the above solution with continues stirring for 20 min for further growth of ZnS/Mn nanparticles resulted in the formation of white precipitate. The precipitate was centrifuged and washed by the distilled water. Obtained powder dry in vacuum at 60 ºC for overnight. The particles were de-agglomerated in pestle-mortar till a very fine powder was obtained.

Synthesis of polypyrrole (PPy): For the synthesis of polypyrrole (PPy), 17.404 g of $FeCl_3$ dissolved in 50 mL distilled water by stirring for 60 min. The solution was then added dropwise to the solution containing 3.099 mL pyrrole monomer in 50 mL deionized water. Immediately, the polymerization was initiated with the formation of black colour precipitates. The stirring was allowed to continue for 24 h. After that obtained precipitates were filtered and washed many time with deionized water. The synthesized polymer was dry in vacuum at 70 ºC for 12 h to get polypyrrole.

Synthesis of polypyrrole capped ZnS/Mn (ZnS/Mn/PPy) nanocomposites: For the synthesis process, 3 g of Mn doped ZnS powder was wetted with 300 µL of pyrrole monomer for 30 min. Deionized water (20 mL) was added to the above solution with continuous stirring for 15 min. To start polymerization, 1.404 g of oxidizing agent ($FeCl_3$) dissolved in 10 mL deionized water was added dropwise to the above solution. The solution was kept in rest after stirring for 24 h. Final solution was filtered and washed with deionized water and dried in vacuum for 2 h at 60 ºC. In this way, ZnS/Mn/PPy composites containing various weight percentages of polypyrrole (4, 8, 12, 15 and 18 wt.%) with 2.4 molar ratio of oxidizing agent to pyrrole were synthesized.

Characterization: The size of the polypyrrole coated Mn doped ZnS nanoparticles was determined by X-ray diffraction (XRD) using (Panalytical's X'Pert Pro) diffractometer. The vibrational spectra of the samples were analyzed by Fourier transform infrared (FT-IR), (Model no. IRAFFINITY- 21CE. Optical characterization was carried out by UV-Vis and photoluminescence (PL) spectroscopy using a Multi-mode micro plate Reader (Synergy H1) hybrid from Bio Tek. To obtain the morphology of the particles high resolution transmission electron microscope (HRTEM) (TECNAI G20 TEM) was used.

RESULTS AND DISCUSSION

X-ray diffraction studies: The XRD spectra of uncapped and PPy capped ZnS/Mn quantum dots showing three diffraction peaks is shown in Fig. 1 which appear at $2\theta = 29.1°$, 48.2° and 57.5° corresponds to (111), (220) and (311) planes, which are well matched with cubic zinc blend structure with JCPDS no. (01-080-0020). The crystallite size of ZnS/Mn and ZnS/Mn/PPy samples with different capping concentration of PPy (4%, 8%, 12% and 15%) was calculated by using Debye Scherrer's formula [22] from high intensity peak.

$$D = \frac{0.94K\lambda}{\beta\cos\theta} \quad (1)$$

where, D = Average particle size, K = 0.9; λ = 1.54 Å; θ = Bragg angle; β = FWHM.

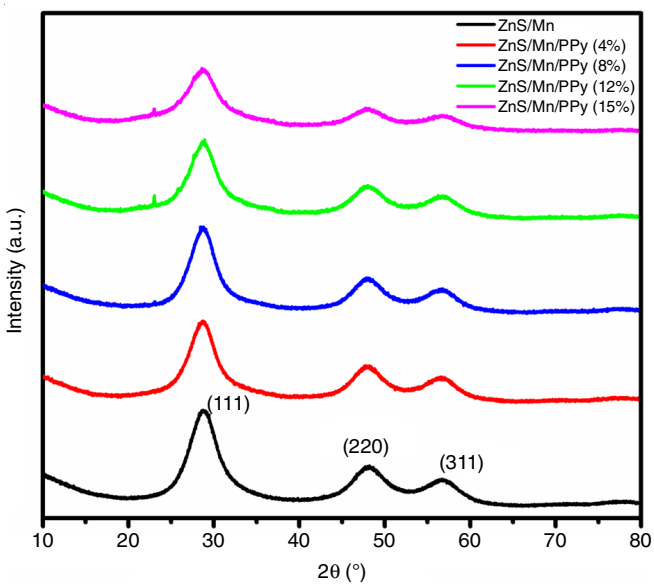

Fig. 1. XRD pattern of ZnS/Mn and ZnS/Mn/PPy quantum dots

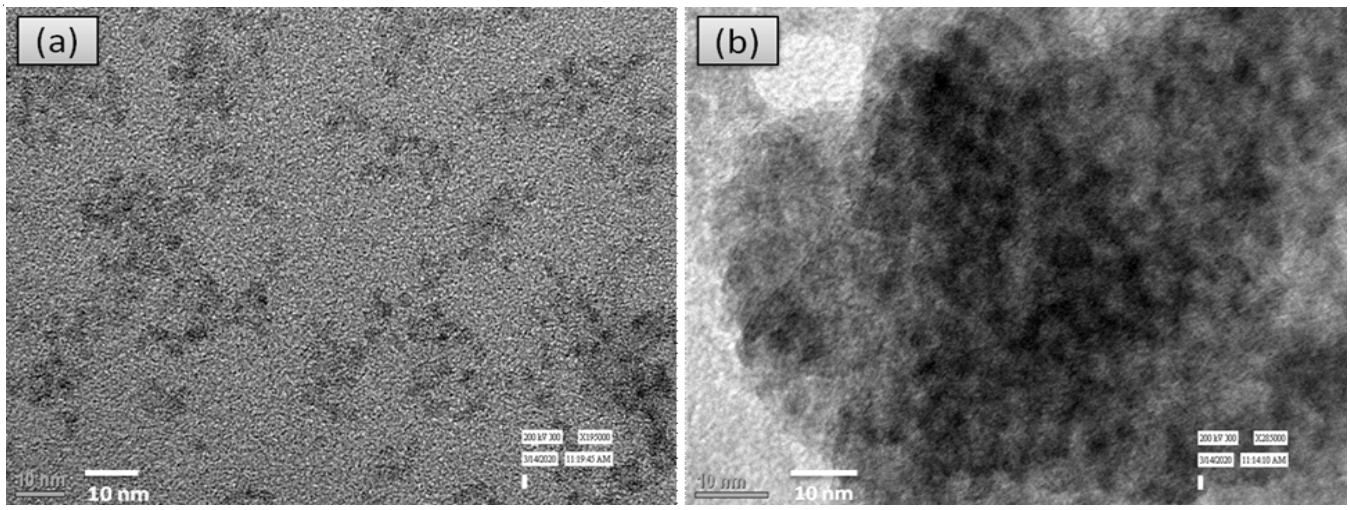

Fig. 2. TEM of (a) ZnS/Mn (b) ZnS/Mn/PPy quantum dots

Average crystalline size of uncapped ZnS/Mn and PPy capped ZnS/Mn nanoparticles calculated by above eqn. 1 is shown in Table-1. It can be concluded that crystalline size of synthesized PPy capped ZnS/Mn quantum dots for various concentrations of PPy are approximate 2 nm, which comes below to Bohr's radius for exciton (2.5 nm for ZnS), As a result, a significant quantum confinement effects expected in these samples.

TABLE-1
LIST OF CRYSTALLITE SIZE

Concentration of capping agent (PPy)	Crystallite size (nm) from (111) peak
0%	2.05
4%	2.10
8%	2.24
12%	1.95
15%	1.51

Transmission electron microscope (TEM) studies: Low and high resolution bright field transmission microscopes were used to get the most accurate information on the morphology of the samples. TEM micrographs of uncapped and PPy capped ZnS/Mn quantum dots are shown in Fig. 2. The sizes of most of the particles range between 2-3 nm, which is identical to the XRD data. The TEM micrographs clearly show that size of the uncapped ZnS nanoparticles and PPy capped ZnS nanoparticles almost same.

FTIR studies: Fig. 3 shows the FTIR spectra of pure PPy and the respective composites containing the PPy, ZnS and Mn nanoparticles. The vibration bands are observed at 3377.36, 2891.3, 1448.54, 1163.08, 740.67 and 617.22 cm^{-1}. These bands revealed the formation of pure PPy. The band observed at 617.22 cm^{-1} may be attributed to the N–H vibrations in polymer [23]. A strong intensity band at 1448.54 cm^{-1} is associated with the C-N stretching mode of vibration in the polypyrrole ring [17]. Whereas, two broad peaks at 740.67 and 1163.08 cm^{-1} are associated with ring deformation of pyrrole and C-N stretch bending respectively [24,25]. On the other hand, a sharp peak at 2891 cm^{-1} arised due to stretching vibration of C–H bond. The occurrence of a wide peak at 3400 cm^{-1} is

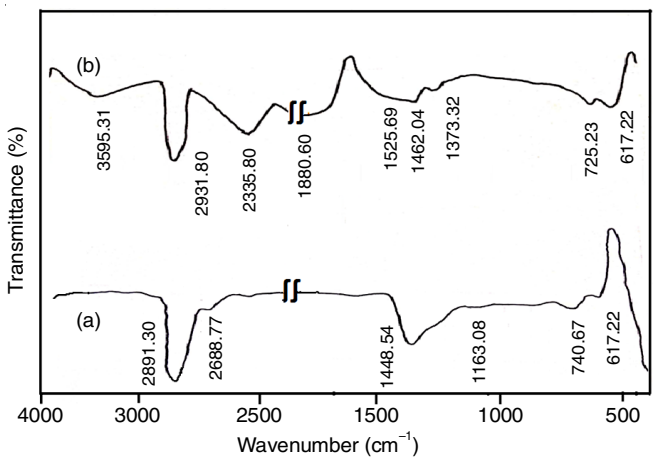

Fig. 3. FTIR pattern of (a) Pure PPy (b) ZnS/Mn/PPy nanoparticles

assigned to the presence of N-H stretching vibrations of pyrrole ring [26]. The spectra for ZnS/Mn/PPy nanocomposites peaks of above functional groups were slightly shift as compared to the pure PPy sample. Peak observed at 740.67cm^{-1}, shift to 725.23 cm^{-1}, 1448.54 cm^{-1} shift to 1462.04 cm^{-1} and 2345.44 cm^{-1} shift to 2335.8 cm^{-1} in the ZnS/Mn/PPy nanocomposites. The shifting of broad peak at 2335.8 cm^{-1} was due to S-H stretching vibrations, which confirmed interaction of hydrogen and sulphur in ZnS/Mn/PPy nanocomposites. Moreover, results indicate that the new bands are appeared in FTIR spectra of ZnS/Mn/PPy nanocomposites which are at 1373.32, 1525, 1880.60, 2931.80 cm^{-1}. The characteristics peak at 1373.32 cm^{-1} assoc-iated with the carboxyl stretching vibrations [27], whereas the other peak at 1525 cm^{-1} assigned to the stretching vibrations of both C-C and C=C bonds [28]. The main peaks in the FTIR analysis at 1880 and 2931 cm^{-1} clearly indicate the formation of PPy capped ZnS/Mn nanoparticles. The major variations in peak positions spectra may be due to certain chemical reactions between PPy and ZnS nanoparticles.

UV-visible studies: Fig. 4 shows the absorption spectra of uncapped and PPy capped ZnS/Mn quantum dots. Absorption edge were measured at wavelength of 295, 300, 325, 320 and 310 nm for uncapped and PPy (4%, 8%, 12% and 15%) capped

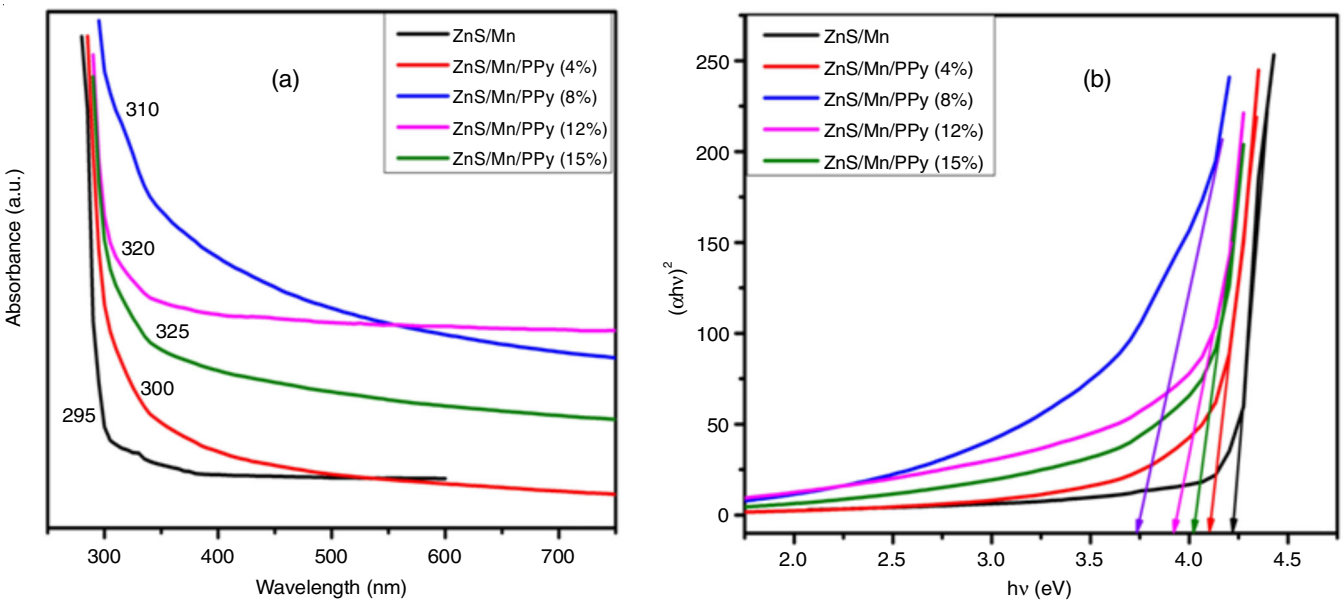

Fig. 4. (a) Absorbance spectra (b) Tauc's plot of unacppped and PPy capped ZnS/Mn samples

ZnS/Mn nanocomposites, respectively (Fig. 4a). The value of the band gap for the direct transition can be fixed by extrapolating the straight line portion of $(\alpha h\nu)^2$ *versus* hν graph for uncapped ZnS/Mn and PPy capped ZnS/Mn nanoparticles which is shown in Fig. 4b. It is clearly observed from Fig. 4b that direct band gap energy of PPy capped ZnS/Mn decreases from 4.21 eV for ZnS/Mn to (4.10 eV, 3.73 eV, 3.92 eV and 4.00 eV) for PPy (4%, 8%, 12% and 15%), respectively. Table-2 shows measured band gap with blue shift for different samples. The absorption spectra of all the samples indicate a significant quantum confinement effect when compared to bulk ZnS, which has a band gap of 3.68 eV. Empirical formula [29] was used for the calculation of particle size of ZnS/Mn and ZnS/Mn/PPy nanoparticles (eqn. 3).

$$2R = \frac{0.1}{0.138 - 0.0002345\lambda_c} \quad (3)$$

where, 2R = particle's diameter, λ_c = absorption edge/absorption discontinuity.

TABLE-2
BLUE SHIFT IN UNCAPPED AND CAPPED ZnS/Mn NANOPARTICLES

Samples	Band gap (eV)	Blue shift (eV)
Uncapped	4.21	0.53
4%	4.10	0.42
8%	3.73	0.05
12%	3.92	0.24
15%	4.00	0.32

The average sizes of the particles calculated according eqn. 3 for ZnS/Mn, ZnS/Mn/PPy (4%, 8%, 12% and 15%) quantum dots were 1.45, 1.47, 1.61, 1.58 and 1.53 nm with λ_c is 295, 300, 325, 320 and 310, respectively. The calculated sizes of all particles in the all samples were less than the limit of exciton Bohr's radius (2.5 nm) [30] hence, observing the quantum confinement effect for ZnS from the present calculations. This means that the particle size changed slightly with capping and the band gap will change.

Photoluminescence studies: The photoluminescence spectra of uncapped and PPy capped ZnS/Mn nanocomposites are shown in Fig. 5. Spectra of uncapped and PPy capped ZnS/Mn quantum dots shows two emission peaks. The emission spectra of all the samples exhibit peak intensities of 308 and 600 nm under ultra violet and orange wavelength, respectively. Fig. 5 demonstrates that when PPy is capped on ZnS/Mn nanoparticles the emission peaks move slightly to a higher wavelength region, resulting in a red shift. The peaks at 308 and 600 nm are arised due to sulphur vacancies and $4T_1$-$6A_1$ transition of Mn, respectively [31]. When compared PPy capped ZnS/Mn samples to uncapped ZnS/Mn quantum dots, both sets of peaks showed a red shift. The results of PL spectra are comparable to the UV-visible data, indicates the ZnS/Mn nanoparticles remained their optical properties even after being capped with PPy. The difference between the spectrum of excitation and

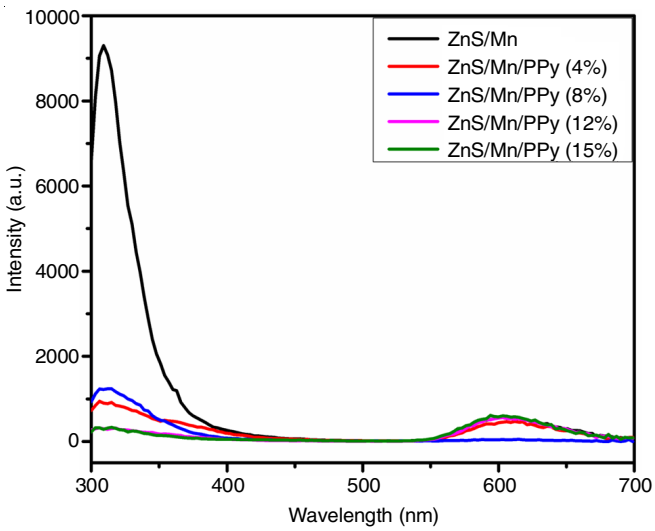

Fig. 5. PL spectra of uncapped and PPy capped ZnS/Mn nanoparticles

emission is shown in Table-3, which indicated that PPy coating on ZnS/Mn nanoaprticles increases further energy levels in the visible range. This is a suggestion for PPy capped ZnS/Mn nanoparticles could be use in optoelectronic applications such as photosensing device [18,32].

TABLE-3
EMISSION DATA FOR THE UNCAPPED ZnS/Mn AND PPy CAPPED ZnS/Mn NANOPARTICLES

Sample	Fixed excitation wavelength (nm)	Emission peak (nm)
Uncapped ZnS/Mn	295	308 and 600
(4%) ZnS/Mn/PPy	300	310 and 604
(8%) ZnS/Mn/PPy	325	311 and 605
(12%) ZnS/Mn/PPy	320	309 and 600
(15%) ZnS/Mn/PPy	310	309 and 595

Conclusion

The polypyrrole functionalized ZnS/Mn particles were synthesized using chemical precipitation method. The size of the particles was found to be nearly 2 nm with different concentration of polypyrrole (PPy) as analyzed by XRD and TEM analyses. The particle size of uncapped and PPy capped ZnS/Mn quantum dots are very near to the exciton Bohr's radius (2.5 nm) reflecting the quantum confinement effect. FTIR spectroscopy confirmed the interaction of PPy and ZnS in ZnS/Mn/PPy nanocomposites. The UV-visible spectrum revealed that the occurrence of blue shift in the peak of absorption and an increase the band gap due to quantum confinement effect. The photoluminescence spectra of uncapped and PPy capped ZnS/Mn nanoparticles confirms two sets of emission peaks corresponds to wavelength of 308 and 600 nm due to sulphur vacancy and $4T_1$-$6A_1$ Mn transition, respectively. The photoluminescence properties of the organically functionalized ZnS/Mn quantum dots make them suitable candidate for the optoelectronic applications.

ACKNOWLEDGEMENTS

The authors are thankful to Maharishi Markandeshwar (deemed to be) University, Mullana, Ambala (Haryana) and Indian Institute of Technology, Roorkee, for providing the research facilities and other support.

CONFLICT OF INTEREST

The authors declare that there is no conflict of interests regarding the publication of this article.

REFERENCES

1. I. Merlin, G. Kavitha, C. Vedhi and A.S. Mohamad, *Mater. Today Proc.*, (2020); https://doi.org/10.1016/j.matpr.2020.06.472
2. K.B. Lin and Y.H. Su, *Appl. Phys. B*, **113**, 351 (2013); https://doi.org/10.1007/s00340-013-5497-z
3. E. Tuncer and E. Turac, *Adv. Polym. Technol.*, **32**, 1 (2013); https://doi.org/10.1002/adv.21373
4. T. Song, J.Y. Cheong, H. Cho, I.D. Kim and D.Y. Jeon, *RSC Adv.*, **9**, 15177 (2019); https://doi.org/10.1039/C9RA01462D
5. R.K. Chandrakar, R.N. Baghel, V.K. Chandra and B.P. Chandra, *Superlattices Microstruct.*, **86**, 256 (2015); https://doi.org/10.1016/j.spmi.2015.07.043
6. P. Sakthivel, K. Kavi Rasu, G.K.D. Prasanna Venkatesan and A. Viloria, *Spectrochim. Acta A Mol. Biomol. Spectrosc.*, **241**, 118666 (2020); https://doi.org/10.1016/j.saa.2020.118666
7. K.K. Rasu, P. Sakthivel and G.P. Venkatesan, *Opt. Laser Technol.*, **130**, 106365 (2020); https://doi.org/10.1016/j.optlastec.2020.106365
8. P. Sakthivel, G.K.D. Prasanna Venkatesan, K. Subramaniam and P. Muthukrishnan, *J. Mater. Sci. Mater. Electron.*, **30**, 11984 (2019); https://doi.org/10.1007/s10854-019-01551-2
9. J. Sharma, A. Gupta and O.P. Pandey, *Ceram. Int.*, **45**, 13671 (2019); https://doi.org/10.1016/j.ceramint.2019.04.061
10. N. Karar, F. Singh and B.R. Mehta, *J. Appl. Phys.*, **95**, 656 (2004); https://doi.org/10.1063/1.1633347
11. A.B. Cruz, Q. Shen and T. Toyoda, *Mater. Sci. Eng. C*, **25**, 761 (2005); https://doi.org/10.1016/j.msec.2005.06.022
12. A. Kaderavkova, L. Loghina, M. Chylii, S. Slang, P. Placek, B. Frumarova and M. Vlcek, *J. Alloys Compd.*, **154**, 814 (2020); https://doi.org/10.1016/j.jallcom.2020.154814
13. H. Van Bui, H.N. Nguyen, N.N. Hoang, T.T. Truong and V. Ben Pham, *IEEE Trans. Magn.*, **50**, 2400504 (2014); https://doi.org/10.1109/TMAG.2014.2300187
14. M. Kuppayee, G.V. Nachiyar and V. Ramasamy, *Appl. Surf. Sci.*, **257**, 6779 (2011); https://doi.org/10.1016/j.apsusc.2011.02.124
15. B. Li, H.-H. Wu, P.-F. Luo, K. Lin, J.-G. Cheng, H.-H. Zhong, Y. Jiang and Y.-W. Lu, *Chem. Phys. Lett.*, **123**, 735 (2019); https://doi.org/10.1021/acs.jpcc.8b10851
16. M. Singhal, J.K. Sharma and S. Kumar, *J. Mater. Sci. Mater. Electron.*, **23**, 1387 (2012); https://doi.org/10.1007/s10854-011-0603-7
17. M. Sookhakian, Y.M. Amin, S. Baradaran, M.T. Tajabadi, A.M. Golsheikh and W.J. Basirun, *Thin Solid Films*, **552**, 204 (2014); https://doi.org/10.1016/j.tsf.2013.12.019
18. D. Bijimol, M.S. Punnoose, B.K. Korah and B. Mathew, *AIP Conf. Proc.*, **2269**, 030002 (2020); https://doi.org/10.1063/5.0019540
19. T. Gan, N. Zhao, G. Yin, M. Tu, J. Liu and W. Liu, *New J. Chem.*, **41**, 13425 (2017); https://doi.org/10.1039/C7NJ02625K
20. J. Osuntokun and P.A. Ajibade, *J. Nanomater.*, **2016**, 3296071 (2016); https://doi.org/10.1155/2016/3296071
21. X.J. Qin, L. Zhao, G.J. Shao and N. Wang, *Thin Solid Films*, **542**, 144 (2013); https://doi.org/10.1016/j.tsf.2013.07.002
22. A. Bala, R. Sehrawat, A.K. Sharma and P. Soni, *J. Mater. Sci.: Mater Electron.* **32**, 16382 (2021); https://doi.org/10.1007/s10854-021-06191-z
23. A. Batool, F. Kanwal, M. Imran, T. Jamil and S.A. Siddiqi, *Synth. Met.*, **161**, 2753 (2012); https://doi.org/10.1016/j.synthmet.2011.10.016
24. N.D. Gupta, D. Banerjee, N.S. Das and K.K. Chattopadhyay, *Colloids Surf. A Physicochem. Eng. Asp.*, **385**, 55 (2011); https://doi.org/10.1016/j.colsurfa.2011.05.044
25. S.K. Mishra, R. Pasricha, A.M. Biradar and Rajesh, *Appl. Phys. Lett.*, **100**, 053701 (2012); https://doi.org/10.1063/1.3681580
26. A. Yussuf, M. Al-Saleh, S. Al-Enezi and G. Abraham, *Int. J. Polym. Sci.*, **2018**, 4191747 (2018); https://doi.org/10.1155/2018/4191747
27. Z. Neisi, Z. Ansari-Asl, S. Jafarinejad-Farsangi, M.E. Tarzi, T. Sedaghat and V. Nobakht, *Colloids Surf. B Biointerfaces*, **178**, 365 (2019); https://doi.org/10.1016/j.colsurfb.2019.03.032
28. L.P. Júnior, D.B.D.S. Silva, M.F. de Aguiar, C.P. de Melo and K.G.B. Alves, *J. Mol. Liq.*, **275**, 452 (2019); https://doi.org/10.1016/j.molliq.2018.11.084
29. M. Rana and P. Chowdhury, *J. Luminesc.*, **206**, 105 (2019); https://doi.org/10.1016/j.jlumin.2018.10.060
30. M. Singhal, J.K. Sharma, H.C. Jeon, T.W. Kang and S. Kumar, *J. Mater. Sci. Mater. Electron.*, **27**, 3003 (2016); https://doi.org/10.1007/s10854-015-4122-9
31. B. Xia, I.W. Lenggoro and K. Okuyama, *Chem. Mater.*, **14**, 4969 (2002); https://doi.org/10.1021/cm020409i
32. A. AL-Osta, A. Alnehia, A.A. Qaid, H.T. Al-Ahsab and A. Al-Sharabi, *Optik*, **214**, 164831 (2020); https://doi.org/10.1016/j.ijleo.2020.164831